Available online at www.sciencedirect.com
ScienceDirect
Journal of Chromatography A, 1142 (2007) 19–31
JOURNAL OF CHROMATOGRAPHY A
www.elsevier.com/locate/chroma

pH transitions in cation exchange chromatographic columns containing weak acid groups

Timothy M. Pabst, Giorgio Carta *

Department of Chemical Engineering, University of Virginia, 102 Engineers' Way, Charlottesville, VA 22904-4741, USA

Available online 15 September 2006

Abstract

Complex pH transitions occur in cation exchange columns used for protein chromatography during equilibration and salt elution steps when the stationary phase contains weak acid groups even if the mobile phase is buffered and the buffering species do not interact with the stationary phase. In this work, we present a local equilibrium model to predict the magnitude and duration of these pH transients. The model equations are solved by the method of characteristics and by numerical simulations using an equilibrium-dispersive model. By incorporating an explicit description of the dissociation of the weakly ionogenic groups in the resin, we show that counterion binding in the column can be predicted for different buffer systems based on a single experimental resin titration curve without having to resort to empirically defined adsorption equilibrium constants. Model predictions based on these assumptions are found to be in excellent agreement with experimental results obtained for three different resins containing varying concentrations of weak acid groups. Four common buffer systems, acetate, citrate, MES, and phosphate are considered with both step and gradient changes in salt concentration at pH 5.5. Each buffer yields a different pH excursion behavior. We demonstrate that when the counterion concentration is kept constant in each of these buffers, which is needed to attain identical protein adsorption behavior, the magnitude of the pH transitions occurring during salt steps is nearly independent of the buffer system. On the other hand, the duration of the pH transitions is smallest for MES suggesting that this buffer system is preferable where pH variations are to be prevented.

Keywords: pH transitions; Weak acid resins; Characteristics; Salts steps; Gradient elution

1. Introduction

Complex pH transitions occur in cation exchange columns during equilibration and salt elution steps when the stationary phase contains weak cation exchange groups such as carboxylates. Substantial pH excursions occur even if the mobile phase is buffered and the buffering species do not interact with the stationary phase; i.e. with neutral and negatively charged buffers. Such pH fluctuations can affect the separation of proteins in both gradient and step elution operations and can require large equilibration volumes. Moreover, if the pH fluctuations are extreme, they can potentially affect pH-sensitive proteins.

Ghose et al. [1] have reported the occurrence of pH transitions during salt concentration steps in a protein chromatography column packed with the stationary phase Fractogel EMD $SO3^-$ from EM Industries (Hawthorne, NY). These authors observed a temporary decrease in the pH during positive salt steps, and a temporary increase in the pH during negative salt steps even if both starting and final solutions were buffered at the same pH. This phenomenon was shown to occur whether or not protein was present and was attributed to a release (or uptake) of protons in exchange for positively charged mobile phase counterions by the resin's sulfonic acid groups. In reality, although the resin used is nominally a strong cation exchanger containing sulfonic acid groups, it also contains a significant number of carboxylic acid groups, likely the result of hydrolysis of its polymethylmethacrylate backbone. On this basis, the authors suggested a direct correlation between pH fluctuations and the amount of weak acid groups in the resin, which varied with exposure of the resin to sodium hydroxide sanitizing solutions. The pH transitions were found to be dependent upon the buffer used, with morpholino-ethane-sulfonic acid (MES) having larger pH swings than phosphate buffer even if the ionic concentration was reportedly the same.

Soto Pérez and Frey [2] have recently reported a theoretical and experimental study of pH transitions in weak anion

* Corresponding author. Tel.: +1 434 924 6281; fax: +1 434 982 2658.
E-mail address: gc@virginia.edu (G. Carta).

0021-9673/$ – see front matter © 2006 Elsevier B.V. All rights reserved.
doi:10.1016/j.chroma.2006.08.066

exchangers. The transient pH changes were opposite to those of Ghose et al. since a weak anion exchanger was used instead of a resin containing weak cation exchanger. As a result, the pH increased for a positive salt concentration step and decreased for a negative step. The theoretical analysis was based on the local equilibrium assumption and considered partitioning or adsorption of all ionic and non-ionic species on the resin phase. Although the model was not specifically solved for weak cation exchangers, Soto Pérez and Frey indicated that their model is generally consistent with the results of Ghose et al., also suggesting the possibility that greater pH transients might occur for buffers like MES if adsorption of uncharged species present in such buffers were to occur.

In this work we develop a local equilibrium model to predict the magnitude and duration of pH transitions in weak cation exchange columns based upon the properties of the resin and the mobile phase buffer. The modeling approach is similar to that of Soto Pérez and Frey and follows the earlier work of Bennett and Helfferich [3] on pH waves in anion exchange columns. There are a few significant differences, however. First, we incorporate an explicit description of the dissociation of the weak ionogenic groups in the resin. We show that counterion binding in the column can be predicted directly based on an experimental titration curve without having to resort to empirically defined adsorption equilibrium constants. Secondly, we neglect adsorption of all buffering species assuming that the only species bound is the counterion. Model predictions based on these assumptions are found to be in excellent agreement with experimental results obtained for three different resins containing varying amounts of weak cation exchange groups using acetate, citrate, MES, and phosphate buffer systems with both step and gradient changes in salt concentration. We show that, for the resins considered in this work, when the counterion concentration is kept constant (which is needed to attain identical protein adsorption behavior on cation exchangers), at pH values between 5.5 and 6.5 the magnitude of the pH transitions is independent of buffer system, provided the initial and final pH values are the same. Conversely, the duration of the pH drop is smallest for MES suggesting that this buffer system is actually preferable if pH transitions are to be minimized.

2. Theoretical development

Modeling pH transitions in columns containing weak acid groups requires a description of both solution and ion exchange equilibria as well as material balances to describe the column dynamics. This development is limited to acetate, citrate, MES, and phosphate buffer systems with NaCl added to modulate the buffer ionic strength. Other buffer systems can be dealt with in a similar manner.

2.1. Solution equilibria

2.1.1. Acetate and MES buffers

For an acetate buffer, solution equilibrium is described by

$$CH_3COOH \Leftrightarrow CH_3COO^- + H^+ \tag{1}$$

with

$$K_a = \frac{C_{CH_3COO^-} C_{H^+}}{C_{CH_3COOH}} \tag{2}$$

The acetate ion concentration is easily obtained from

$$C_{CH_3COO^-} = \frac{K_a C_A}{K_a + C_{H^+}} \tag{3}$$

where $C_A = C_{CH_3COOH} + C_{CH_3COO^-}$. The concentrations of the charged species in solution are bound by the electroneutrality condition, which is expressed by

$$C_{Na^+} + C_{H^+} = C_{CH_3COO^-} + C_{OH^-} + C_{Cl^-} \tag{4}$$

Finally, combining Eqs. (3) and (4) with the ionic product of water, $K_w = C_{H^+} C_{OH^-}$, yields

$$C_{Na^+} + C_{H^+} = \frac{K_a C_A}{K_a + C_{H^+}} + \frac{K_w}{C_{H^+}} + C_{Cl^-} \tag{5}$$

Given sodium, chloride and total acetate concentrations, this cubic equation can be solved for C_{H^+}. For typical conditions the difference $C_{Na^+} - C_{Cl^-}$ is much greater than either C_{H^+} or C_{OH^-}. In this case, Eq. (5) can be simplified yielding

$$C_{H^+} = K_a \left(\frac{C_A}{C_{Na^+} - C_{Cl^-}} - 1 \right) \tag{6}$$

The MES buffer dissociates according to

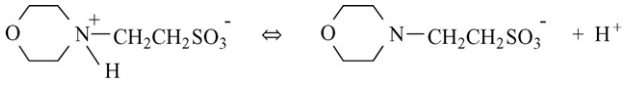

(7)

Therefore, the above equations apply to MES as well, with the zwitterionic form of MES used in place of CH_3COOH.

2.1.2. Citrate and phosphate buffers

Multiple dissociations need to be considered for these buffers and can be handled as follows. For citrate the solution equilibria are described by

$$C_6H_8O_7 \Leftrightarrow C_6H_7O_7^- + H^+ \tag{8}$$

$$C_6H_7O_7^- \Leftrightarrow C_6H_6O_7^{2-} + H^+ \tag{9}$$

$$C_6H_6O_7^{2-} \Leftrightarrow C_6H_5O_7^{3-} + H^+ \tag{10}$$

with

$$K_{a1} = \frac{C_{C_6H_7O_7^-} C_{H^+}}{C_{C_6H_8O_7}} \tag{11}$$

$$K_{a2} = \frac{C_{C_6H_6O_7^{2-}} C_{H^+}}{C_{C_6H_7O_7^-}} \tag{12}$$

$$K_{a3} = \frac{C_{C_6H_5O_7^{3-}} C_{H^+}}{C_{C_6H_6O_7^{2-}}} \tag{13}$$

At moderately acidic or near neutral pH – typical of practical operating conditions – all three reactions are relevant and we obtain

$$C_{C_6H_8O_7} = \frac{C_C}{1 + (K_{a1}/C_{H^+}) + (K_{a1}K_{a2}/(C_{H^+})^2) + (K_{a1}K_{a2}K_{a3}/(C_{H^+})^3)} \quad (14)$$

$$C_{C_6H_7O_7^-} = \frac{C_C K_{a1}/C_{H^+}}{1 + (K_{a1}/C_{H^+}) + (K_{a1}K_{a2}/(C_{H^+})^2) + (K_{a1}K_{a2}K_{a3}/(C_{H^+})^3)} \quad (15)$$

$$C_{C_6H_6O_7^{2-}} = \frac{C_C K_{a1}K_{a2}/(C_{H^+})^2}{1 + (K_{a1}/C_{H^+}) + (K_{a1}K_{a2}/(C_{H^+})^2) + (K_{a1}K_{a2}K_{a3}/(C_{H^+})^3)} \quad (16)$$

$$C_{C_6H_5O_7^{3-}} = \frac{C_C K_{a1}K_{a2}K_{a3}/(C_{H^+})^3}{1 + (K_{a1}/C_{H^+}) + (K_{a1}K_{a2}/(C_{H^+})^2) + (K_{a1}K_{a2}K_{a3}/(C_{H^+})^3)} \quad (17)$$

where $C_C = C_{C_6H_8O_7} + C_{C_6H_7O_7^-} + C_{C_6H_6O_7^{2-}} + C_{C_6H_5O_7^{3-}}$. Considering the electroneutrality condition

$$C_{Na^+} + C_{H^+} = C_{C_6H_7O_7^-} + 2C_{C_6H_6O_7^{2-}} + 3C_{C_6H_5O_7^{3-}} + C_{OH^-} + C_{Cl^-} \quad (18)$$

we obtain

$$C_{Na^+} + C_{H^+} = C_C \frac{(K_{a1}/C_{H^+}) + 2(K_{a1}K_{a2}/(C_{H^+})^2) + 3(K_{a1}K_{a2}K_{a3}/(C_{H^+})^3)}{1 + (K_{a1}/C_{H^+}) + (K_{a1}K_{a2}/(C_{H^+})^2) + (K_{a1}K_{a2}K_{a3}/(C_{H^+})^3)} + \frac{K_w}{C_{H^+}} + C_{Cl^-} \quad (19)$$

For typical conditions where $C_{Na^+} - C_{Cl^-} >> C_{H^+}$ or C_{OH^-}, Eq. (19) reduces to a cubic with respect to C_{H^+}.

The phosphate buffer equilibria are described by

$$H_3PO_4 \Leftrightarrow H_2PO_4^- + H^+ \quad (20)$$

$$H_2PO_4^- \Leftrightarrow HPO_4^{2-} + H^+ \quad (21)$$

$$HPO_4^{2-} \Leftrightarrow PO_4^{3-} + H^+ \quad (22)$$

Thus, the above equations apply to phosphate buffers as well, with the phosphate species replacing the similarly charged citrate species.

2.1.3. Dissociation constants

The pK_a values recommended by Beynon and Easterby [4] for the buffers used in this work are given in Table 1 at 298 K and infinite dilution. Corrected values accounting for solution ionic strength can be obtained from the extended Debye–Huckel relationship proposed by Davies [5]

$$\log \gamma_i = -z_i^2 \left(\frac{A\sqrt{I}}{1+\sqrt{I}} - bI \right) \quad (23)$$

The following expression is obtained for the corrected pK_a

$$pK'_a = pK_a + 2(z_a - 1)\left(\frac{A\sqrt{I}}{1+\sqrt{I}} - bI \right) \quad (24)$$

where I is the ionic strength, A is a constant that incorporates temperature effects ($A = 0.5114$ at 298 K), b is a buffer-dependent parameter, and z_a is the net charge of the conjugate acid species (0 for acetate and MES and 0, −1, and −2 for citrate and phosphate). The values of the constant b used in this work were as follows. For acetate and pK_{a2} of phosphoric acid, we fitted Eq. (24) to the experimental pK_a in solutions containing NaCl reported by Partanen and Covington [6–8]. Since NaCl is the principal electrolyte in our case, its concentration largely determines the ionic strength. The fitted values of b were 0.16 and 0.07 for acetate and the pK_{a2} of phosphate, respectively. For citrate, MES, and the remaining dissociations of phosphate, since experimental values are not readily available, we used $b = 0.1$ as suggested by Beynon and Easterby [4]. The previous equations for solution equilibria can be used at different ionic strengths by replacing K_a with K'_a.

2.2. Ion exchange equilibria

We consider two semiempirical descriptions of the dissociation behavior of the weakly acidic ionogenic groups in the resin. The first follows the formulation of Helfferich [9] and assumes that the ionogenic groups dissociate according to

$$RH \Leftrightarrow R^- + H^+ \quad (25)$$

where

$$K = \frac{q_{R^-} q_{H^+}}{q_{RH}} \quad (26)$$

is an apparent dissociation constant and the q_i's represent resin-phase concentrations. As pointed out by Helfferich, the pH in the resin phase is different from the pH in the solution. When the

Table 1
Buffer pK_a-values and calculated concentrations of buffer solutions containing 0.02 M Na^+ at pH 5.5 and 298 K

Buffer species	pK_a values [4]	Buffer concentration with no added NaCl (M)	Buffer concentration with 0.5 M NaCl added (M)
Acetate	4.76	0.0232	0.0229
Citrate	3.13, 4.76, 6.40	0.0095	0.0083
MES	6.21	0.1091	0.0907
Phosphate	2.15, 7.21, 12.3	0.0194	0.0188

resin is immersed in a solution containing sodium ions, solution and resin phase pH's are related to each other by [9]

$$q_{H^+} = \frac{C_{H^+}}{C_{Na^+}} q_{Na^+} \tag{27}$$

From Eqs. (26) and (27) we obtain

$$K = \frac{q_{R^-} q_{Na^+} C_{H^+}}{(q_R - q_{R^-}) C_{Na^+}} \tag{28}$$

where $q_R = q_{RH} + q_{R^-}$ is the total concentration of weak acid groups. According to Helfferich, as long as the resin is at least partially converted to the Na^+ form, the concentration of free H^+ in the resin is insignificant. For these conditions, $q_{Na^+} \sim q_{R^-}$ and

$$K = \frac{q_{Na^+}^2 C_{H^+}}{(q_R - q_{Na^+}) C_{Na^+}} \tag{29}$$

or

$$q_{Na^+} = \frac{1}{2}\left[-\frac{K C_{Na^+}}{C_{H^+}} + \sqrt{\left(\frac{K C_{Na^+}}{C_{H^+}}\right)^2 - 4 q_R \frac{K C_{Na^+}}{C_{H^+}}} \right] \tag{30}$$

The values of K and q_R can be determined experimentally by titrating a resin sample that has been equilibrated with a salt solution at low pH. Because of the resin's buffering capacity, the pH increases gradually reaching a plateau when the ionogenic groups are completely converted to the Na^+ form. Following Helfferich, at 50% conversion ($q_{Na^+} = 0.5 q_R$), Eq. (29) yields

$$K = \frac{1}{2} \frac{q_R C_{H^+}}{C_{Na^+}} \tag{31}$$

or

$$pK = pH + \log C_{Na^+} - \log \frac{q_R}{2} \tag{32}$$

Thus, the resin's apparent pK value can be determined experimentally by measuring q_R and the pH at which the resin is half converted to the Na^+ form. Alternatively, pK and q_R can be determined simultaneously by matching experimental and theoretical potentiometric titration curves based on Eq. (30).

The second description of weak acid group dissociation follows the general model of Stoyanov and Righetti [10] for the dissociation of a polyvalent acid. This approach assumes the resin contains n groups capable of parallel dissociations with dissociation constants K_1, K_2, …, K_n. The general result is as follows

$$q_{Na^+} = \frac{q_R}{n} \frac{\sum_{i=1}^{n} i q_{H^+}^{n-i} \prod_{j=1}^{i} K_j}{\left[q_{H^+}^n + \sum_{j=1}^{n} q_{H^+}^{n-j} \prod_{k=1}^{j} K_k \right]} \tag{33}$$

which is combined with Eq. (27) to calculate q_{Na^+}. This equation reduces to Eq. (30) when $n = 1$. For $n = 2$ and 3, cubic and quartic equations must be solved, respectively, to obtain q_{Na^+}. As before, the resin's pK-values and q_R can be obtained by fitting experimental titration curves based on Eq. (33).

2.3. Column dynamics

Using sodium acetate buffer solutions as an example, the dynamic behavior of a weak cation exchange column subject to a change in NaCl concentration can be determined by combining the solution and ion exchange equilibrium relationships discussed above with the following material balances

$$\varepsilon \frac{\partial C_{Na^+}}{\partial t} + (1-\varepsilon) \frac{\partial \bar{q}_{Na^+}}{\partial t} + \varepsilon \nu \frac{\partial C_{Na^+}}{\partial z} = 0 \tag{34}$$

$$\varepsilon \frac{\partial C_{Cl^-}}{\partial t} + (1-\varepsilon) \frac{\partial \bar{q}_{Cl^-}}{\partial t} + \varepsilon \nu \frac{\partial C_{Cl^-}}{\partial z} = 0 \tag{35}$$

$$\varepsilon \frac{\partial C_A}{\partial t} + (1-\varepsilon) \frac{\partial \bar{q}_A}{\partial t} + \varepsilon \nu \frac{\partial C_A}{\partial z} = 0 \tag{36}$$

where $\bar{q}_i = \varepsilon_p C_i + (1-\varepsilon_p) q_i$. These equations assume plug flow and neglect axial dispersion. They also apply to citrate, MES, and sodium phosphate buffers, simply replacing C_A with C_C, C_M, or C_P, respectively. We solve these equations using the method of characteristics assuming local equilibrium with the further assumption that only sodium is bound to the resin; therefore $\bar{q}_{Cl^-} = \varepsilon_P C_{Cl^-}$ and $\bar{q}_A = \varepsilon_P C_A$. This assumption is reasonable as the latter species are neutral or carry the same charge as the resin. With this simplification, the characteristic velocities of Cl^- and buffering species (A or C, M, P) are given by

$$v_{c_{Cl^-}} = v_{c_A} = \frac{1}{1 + \phi \varepsilon_P} \tag{37}$$

where $\phi = (1-\varepsilon)/\varepsilon$. For sodium ion, the characteristic velocity depends on whether we have simple or shock waves. For simple waves, we have

$$v_{c_{Na^+}} = \frac{v}{1 + \phi \left[\varepsilon_P + (1-\varepsilon_P)(dq_{Na^+}/dC_{Na^+}) \right]} \tag{38}$$

with

$$\frac{dq_{Na^+}}{dC_{Na^+}} = \frac{\partial q_{Na^+}}{\partial C_{Na^+}} + \frac{\partial q_{Na^+}}{\partial C_{Cl^-}} \frac{dC_{Cl^-}}{dC_{Na^+}} + \frac{\partial q_{Na^+}}{\partial C_A} \frac{dC_A}{dC_{Na^+}} \tag{39}$$

Conversely, for shock waves we have

$$v_{s_{Na^+}} = \frac{v}{1 + \phi \left[\varepsilon_P + (1-\varepsilon_P) \frac{q'_{Na^+} - q''_{Na^+}}{C'_{Na^+} - C''_{Na^+}} \right]} \tag{40}$$

where $'$ and $''$ represent values upstream and downstream of the shock front, respectively. In both cases, q_{Na^+} is given by the appropriate solution and ion exchange equilibrium relations, i.e. Eq. (6) for acetate and MES or Eq. (19) for citrate and phosphate, each combined with Eqs. (30) or (33).

Coherent, stable concentration waves generated in response to changes in feed composition can be determined from these equations by setting the characteristic or shock velocities equal for all components [3,11,12]. As an example, we consider initially the case where the total concentration of buffering species (C_A, C_C, C_M, or C_P) is kept constant, and only the NaCl concentration is changed from zero to a finite value. In this case, the solution can be represented on the hodograph plane, C_{Cl^-}

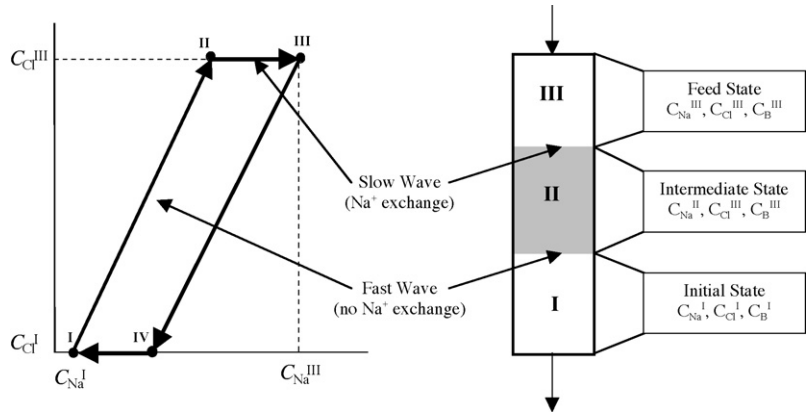

Fig. 1. Hodograph plane and corresponding states during salt steps. Points I and III represent the NaCl-free and high salt buffers, respectively. Point II and IV represent intermediate states during positive and negative salt steps, respectively.

versus C_{Na^+}, shown in Fig. 1. Points I and III represent the initial (NaCl-free) and final (high salt) states in the column, while points II represents an intermediate state. For each point there are two coherent paths shown by thick lines. Since Cl^- is assumed to be excluded from the resin phase ($\partial q_{Cl^-}/\partial C_{Na^+} = 0$), one of the paths has a zero slope. The other must satisfy the equality

$$v_{c_{Cl^-}} = v_{c_{Na^+}} \tag{41}$$

As a result, the coherent path from I to III passes through an intermediate state represented by point II. Eq. (41) yields

$$q^{I}_{Na^+} = q^{II}_{Na^+} \tag{42}$$

This path corresponds to a fast wave through the column with no exchange of sodium between the stationary phase and the mobile phase. Considering Eq. (30), we also have

$$\left(\frac{KC_{Na^+}}{C_{H^+}}\right)^{I} = \left(\frac{KC_{Na^+}}{C_{H^+}}\right)^{II} \tag{43}$$

which shows that, as long as K is constant, an increase in sodium from state I to state II must be accompanied by an increased concentration of H^+, thus temporarily lowering the pH of the solution. To obtain a quantitative result for the acetate and MES systems Eq. (6) can be combined with Eq. (43) yielding

$$\frac{C^{II}_{Na^+}}{C^{I}_{Na^+}} = \frac{K^{II}_a}{K^{I}_a}\frac{C^{II}_{Na^+} - C^{II}_{Cl^-} - C^{II}_A}{C^{I}_{Na^+} - C^{I}_{Cl^-} - C^{I}_A}\frac{C^{I}_{Na^+} - C^{I}_{Cl^-}}{C^{II}_{Na^+} - C^{II}_{Cl^-}} \tag{44}$$

Knowing the initial state ($C^{I}_{Na^+}, C^{I}_{Cl^-}, C^{I}_A$) and the final state ($C^{II}_{Cl^-} = C^{III}_{Cl^-}, C^{II}_A = C^{III}_A$), this equation can be solved for $C^{II}_{Na^+}$. Finally, the solution pH ($= -\log \gamma_{H^+} C_{H^+}$) be calculated using the combined results from Eqs. (6), (23), and (44). The same approach can be used for the citrate and phosphate buffer systems solving for C_{H^+} with Eq. (19).

It is noteworthy that the magnitude of the predicted pH drop is independent of q_R, the resin's pK value, and, except for the dependence on ionic strength, the buffer's pK_a. The duration of the pH drop and the shape of the transition to the feed pH value are, however, heavily dependent on all three parameters and can be determined as follows. The fast wave has a velocity v_{cCl^-}. Thus, state II emerges from the column in $\varepsilon(1+\phi\varepsilon_p)$ column volumes. The rest of the solution follows the path from II to III, along which both C_{Cl^-} and C_A are constant. This path consists of a plateau at II followed by a simple wave with characteristic velocity

$$v_{c_{Na^+}} = \frac{v}{1+\phi\left[\varepsilon_p + (1-\varepsilon_p)(\partial q_{Na^+}/\partial C_{Na^+})_{C^{II}_{Cl^-}, C^{II}_A}\right]} \tag{45}$$

if $v_{c_{Na^+}}$ decreases from II to III. Alternatively, if $v_{c_{Na^+}}$ increases from II to III, the path consists of a plateau at II followed by a shock from II to III with shock velocity

$$v_{s_{Na^+}} = \frac{v}{1+\phi\left[\varepsilon_p + (1-\varepsilon_p)(q^{II}_{Na^+} - q^{III}_{Na^+})/(C^{II}_{Na^+} - C^{III}_{Na^+})_{C^{II}_{Cl^-}, C^{II}_A}\right]} \tag{46}$$

A situation where the path from II to III consists of a shock followed by a gradual wave is also possible when $v_{c_{Na^+}}$ initially increases and then decreases from II to III. The same equations apply to the citrate and phosphate systems. In both cases, analytical evaluation of the derivative $\partial q_{Na^+}/\partial C_{Na^+}$ from Eq. (30) or (33) and either (6) or (19) is cumbersome. However, values of the derivative are readily obtained numerically by taking small C_{Na^+} increments. The result depends on the initial and final states and may be qualitatively and quantitatively different for the different buffers and resins. Illustrative examples are given below in comparison with experimental data.

It should be noted that the same procedure also applies even if both the NaCl and buffering species concentrations are varied simultaneously in the feed as long as the assumption holds true that neither Cl^- nor the buffering species are adsorbed.

For the case of a negative salt step from III to I (see Fig. 1), a similar approach is followed. In this case, the coherent path passes through a different intermediate state, denoted by IV, but corresponding to a fast wave with the same velocity $v_{cCl^-} = v_{cA}$.

The sodium concentration at point IV can be found by solving

$$\frac{C^{IV}_{Na^+}}{C^{III}_{Na^+}} = \frac{K^{IV}_a}{K^{III}_a}\frac{C^{IV}_{Na^+} - C^{IV}_{Cl^-} - C^{IV}_A}{C^{III}_{Na^+} - C^{III}_{Cl^-} - C^{III}_A}\frac{C^{III}_{Na^+} - C^{III}_{Cl^-}}{C^{IV}_{Na^+} - C^{IV}_{Cl^-}} \quad (47)$$

Since at state IV, $C^{III}_{Na^+} < C^{IV}_{Na^+}$ and $C^{IV}_{Cl^-} = C^{I}_{Cl^-}$, $C^{IV}_A = C^{I}_A$, the solution pH must temporarily increase. Eq. (47) applies to the MES system as well by replacing the C_A with C_M. The citrate and phosphate system are more complex, but can be solved following the same approach. As before, the path from IV to I, with constant chloride and total buffer species concentrations, can consist of either a plateau at IV followed by a simple wave to I if $v_{c_{Na^+}}$ decreases or a plateau followed by a shock from IV to I if $v_{c_{Na^+}}$ increases.

3. Experimental

3.1. Stationary phases

Three cation exchangers with the properties summarized in Table 2 were used to validate the model developed in this work. Resins A and B were obtained from Bio-Rad Laboratories Inc. (Hercules, CA). Resin A is based on a methylmethacrylate/acrylamido matrix similar to the BRX-S media studied by Hunter and Carta [13]. The resin contains sulfonic acid groups (SP) along with a significant amount of carboxylic acid groups resulting from the alkaline hydrolysis of the resin's backbone after prolonged exposure to concentrated NaOH at high temperatures. Resin B is based on a SP-type crosslinked polyacrylamido matrix and contains a substantially reduced concentration of weak acid groups compared to resin A. Finally, Resin C is SP-Sepharose FF (GE Healthcare, Piscataway, NJ), an agarose based strong cation exchanger with minimal weak acid group content.

3.2. Chemicals and buffers

pH 5.5 buffer solutions containing a fixed Na^+ concentration were prepared as follows using ACS grade chemicals from Fisher Scientific (Fair Lawn, NJ) and Sigma Chemical Company (St. Louis, MO). Acetate buffers were prepared by dissolving sodium acetate in water and adjusting the pH with concentrated acetic acid. Phosphate buffers were prepared by dissolving anhydrous Na_2HPO_4 in water and adjusting the pH with concentrated phosphoric acid. Citrate buffers were prepared by dissolving tribasic sodium citrate in water and adjusting the pH with citric acid. For MES buffers, a NaOH solution with the desired Na^+ concentration was prepared and the pH was adjusted by adding MES to the solution. All four buffers were prepared with identical sodium concentration, since the latter is the main determinant of protein retention in cation exchange chromatography. Buffer solutions containing NaCl were prepared as described above, however, the pH was adjusted with the correct acid only after the NaCl was added. Since ionic strength affects the buffer pK_a's, the amount of acid added was different from that added to the buffers without NaCl. Table 1 summarizes the compositions of the four buffers studied. After preparation, each buffer was degassed by vacuum filtering although degassing did not seem to have a significant effect on the pH transients suggesting that the amount of dissolved carbon dioxide was likely small in comparison with the buffer concentrations.

Table 2
Summary of resin properties

Property	Resin A	Resin B	Resin C
Particle size[a] (μm)	70	70	90
Extraparticle porosity, ε[b]	0.31	0.31	0.35
Intraparticle porosity, ε_p[c]	0.76	0.76	0.88
Weak acid group content[d]	170	25	5
Strong acid group content[d]	140	145	195
Total acid group content[d]	310	170	200
pK_1[e]	5.2	6.4	3.0
pK_2[e]	6.5	8.3	7.0

[a] Manufacturer data.
[b] Based on retention of blue dextran and pressure drop.
[c] Based on retention of glucose.
[d] Acid group contents are given in μmol/ml packed column. The q-values in μmol/ml resin phase are obtained from the values given by dividing them by the quantity $(1-\varepsilon)(1-\varepsilon_p)$.
[e] pK-values for the dissociation of weak acid groups obtained by fitting Eq. (33) with $n=2$.

3.3. Resin titrations

Potentiometric titrations were conducted as follows. A sample of each resin (~1 ml) was flow packed in 0.5 cm × 5 cm Tricorn™ 5/50 column (GE Healthcare, Piscataway, NJ) at 5 ml/min for resins A and B and 2 ml/min for resin C and equilibrated with 0.1 M NaCl adjusted to pH 4 with HCl. The resin sample was then extruded from the column into 25 ml of 0.1 M NaCl at pH 4, and titrated with standardized NaOH while monitoring the pH. Starting with a salt concentration of 0.1 M and a pH of 4 ensures that only the weak acid groups are titrated, as the sulfonic acid groups start off completely in the sodium form.

The total ion exchange capacity was determined by equilibrating a sample of each resin (~1 ml) with 0.1 N HCl in a Tricorn™ column packed as described above. After washing with de-ionized water, the resin sample was extruded from the column and added to 25 ml of 0.5 M NaCl containing 0.05 M NaOH. After equilibration, a sample of the supernatant was titrated with standardized HCl to determine the amount of NaOH consumed which, in turn, is proportional to the resin's total ionic capacity. The concentration of strong acid groups was determined by subtracting the concentration of weak acid groups from the concentration of total acid groups.

3.4. Column pH transients

All step and gradient experiments were conducted with an AKTA Explorer 10 system (GE Healthcare, Piscataway, NJ) with each resin flow packed in a 1 cm × 10 cm Tricorn™ column. The extraparticle void fraction, ε, was determined from the column pressure with the Carman-Kozeny equation for resins A and B and from the elution volume of blue dextran for resin C. The intraparticle porosity, ε_p, was determined from the retention of glucose and was 0.76 for resins A and B and 0.88 for resin

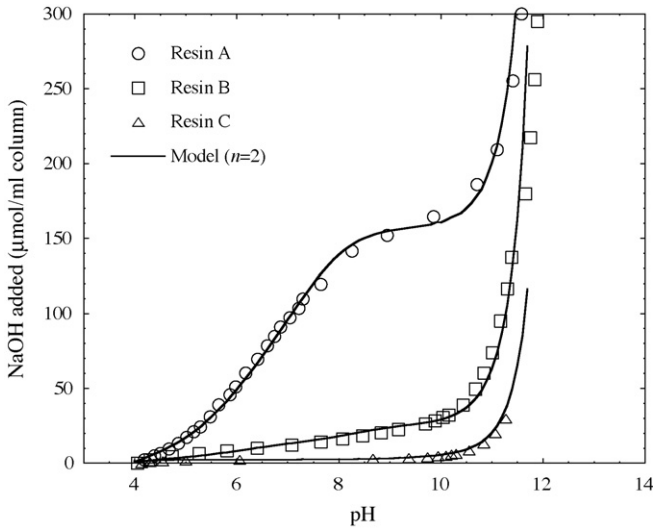

Fig. 2. Experimental and theoretical titration curves for resins A, B, and C equilibrated in 0.1 M NaCl at pH 4. The lines are based on Eq. (33) with $n = 2$ and pK-values in Table 2.

C. Conductivity and pH were monitored with the AKTA system instrumentation. However, accurate pH measurements could only be obtained by collecting fractions and measuring off-line with a calibrated pH meter (Orion, Cambridge, MA). Conductivity traces were converted to sodium concentration for a qualitative comparison with the model predictions. However, the experimental sodium trace obtained this way is only an approximation since the conductivity is also affected by the buffering species concentration, which is dependent upon the pH.

Experiments were conducted with buffers containing 0.02 and 0.1 M sodium concentrations. In each salt step experiment, the resin was equilibrated with buffer containing no salt, and then exposed to 0.5 M NaCl buffer, followed by a step back down to the salt free buffer. Step runs were conducted at 4 ml/min (∼300 cm/h) for resin A and 1 ml/min (∼75 cm/h) for resins B and C. Gradient runs were conducted at 4 ml/min (∼300 cm/h) with a 0–0.5 M NaCl gradient in 21 column volumes.

4. Results and discussion

4.1. Resin titrations

The results of the titration experiments are shown in Fig. 2. The amount of NaOH added increases gradually at first and then reaches a plateau, when all the weak acid groups have been converted to the sodium form. Beyond this point, the titration curves rise sharply since the resin has lost all its buffering capacity. Resin A has the highest concentration of weak acid groups (1020 μmol/ml resin phase ∼170 μmol/ml packed column) while resins B and C have much lower concentrations. Theoretical curves based on Eq. (33) are also shown in Fig. 2 fitted to the data by adjusting n and the pK-values. The quality of the fit improved substantially as n was increased from 1 to

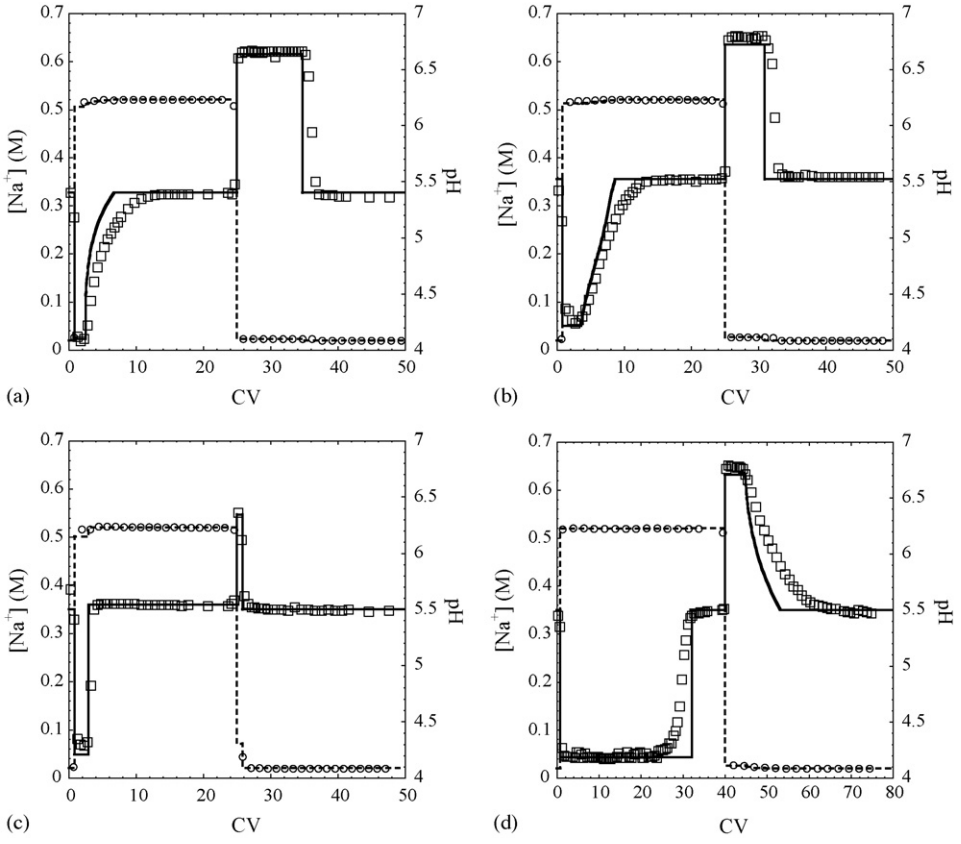

Fig. 3. Experimental and predicted pH and sodium concentration profiles for positive and negative 0–0.5 M NaCl steps with resin A using buffers containing 0.02 M Na^+ at pH 5.5. (a) Acetate, (b) citrate, (c) MES, and (d) phosphate. (◯) Exp. Na^+, (□) exp. pH, (- - - -) model Na^+, (—) model pH.

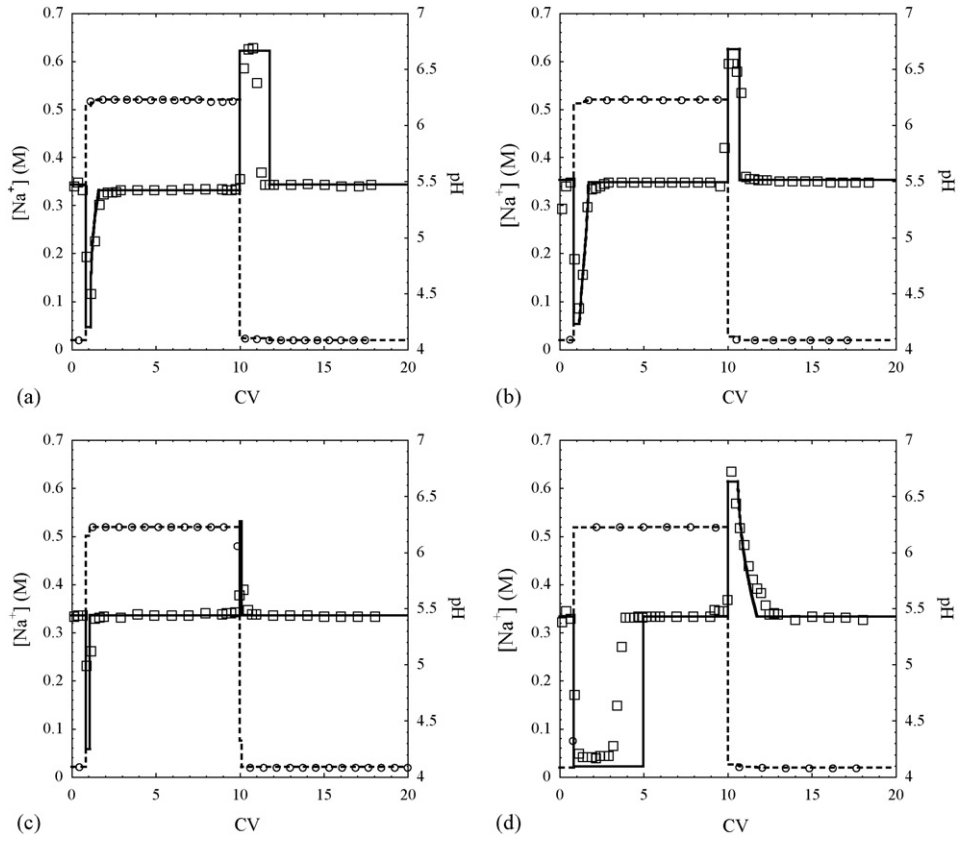

Fig. 4. Experimental and predicted pH and sodium concentration profiles for positive and negative 0–0.5 M NaCl steps with resin B using buffers containing 0.02 M Na^+ at pH 5.5. (a) Acetate, (b) citrate, (c) MES, and (d) phosphate. (◯) Exp. Na^+, (□) exp. pH, (- - - -) model Na^+, (—) model pH.

2. However, the improvement was insignificant when n was increased further. Thus, the best-fit values of pK_1 and pK_2 for $n = 2$ were used for all subsequent calculations and are given in Table 2.

4.2. pH transitions for salt steps

Figs. 3 and 4 show experimental and predicted pH transitions for resins A and B, respectively, in response to 0–0.5 M NaCl steps with acetate, citrate, MES, and phosphate buffers containing 0.02 M Na^+ at pH 5.5. Fig. 5 shows the corresponding results for resin A using the same buffers but containing 0.1 M Na^+. Finally, Fig. 6 shows the results for resin C with acetate buffers containing 0.02 and 0.1 M Na^+ at the same pH. As expected, the pH decreases with a positive salt step and increases with a negative salt step. In all cases, the model correctly predicts the shape of the pH waves. For runs conducted with the citrate and acetate buffers with resins A and B, simple (gradual) waves are predicted during positive salt steps and shock waves are predicted during the step down for both 0.02 and 0.1 M sodium buffers. For the phosphate buffer in both stationary phases shock waves are predicted for steps up, while gradual waves are predicted for the steps down. Finally, in the case of MES buffers, shock waves are predicted for both the step up and down. The model not only correctly predicts the shape of the wave, but also the extremes and duration of the pH transitions. All model calculations were based on the local equilibrium assumption. Thus, dispersion effects are completely neglected. It should be noted that the only fitted parameters are those derived from the resin titration. Therefore, all predictions with the four different buffers are based on exactly the same resin titration curves.

For all four buffers both resins A and B exhibit pH drops of approximately 1.4 with a buffer sodium concentration of 0.02 M and 0.7 pH units with a buffer sodium concentration of 0.1 M, nearly irrespective of buffer type. This experimental behavior is consistent with the model prediction that the magnitude of the pH drop is essentially independent of q_R, the resin's pK value, and the buffer's pK_a with the exception of the effect of ionic strength on activity coefficients. This is also true for the magnitude of the pH rise during a negative salt step which was approximately constant at 1.3 pH units for the 0.02 M sodium buffers and 0.7 pH units for the 0.1 M sodium buffers. The variations between different buffers as well as for the same buffer with different salt concentrations are due largely to the dependence of pK_a on the buffer's ionic strength. In the case of resin C, the magnitudes of the experimental pH transitions are somewhat smaller than predicted. In this case, however, because of the small concentration of weak acid groups, the pH transients have a very short duration. It is likely that dispersive effects, which are not accounted for in the model, diluted the experimental profiles resulting in measured pH transitions that are smaller in magnitude than predicted.

Unlike the magnitude, the duration of the pH transitions is directly dependent on q_R and the resin pK as well as the buffer

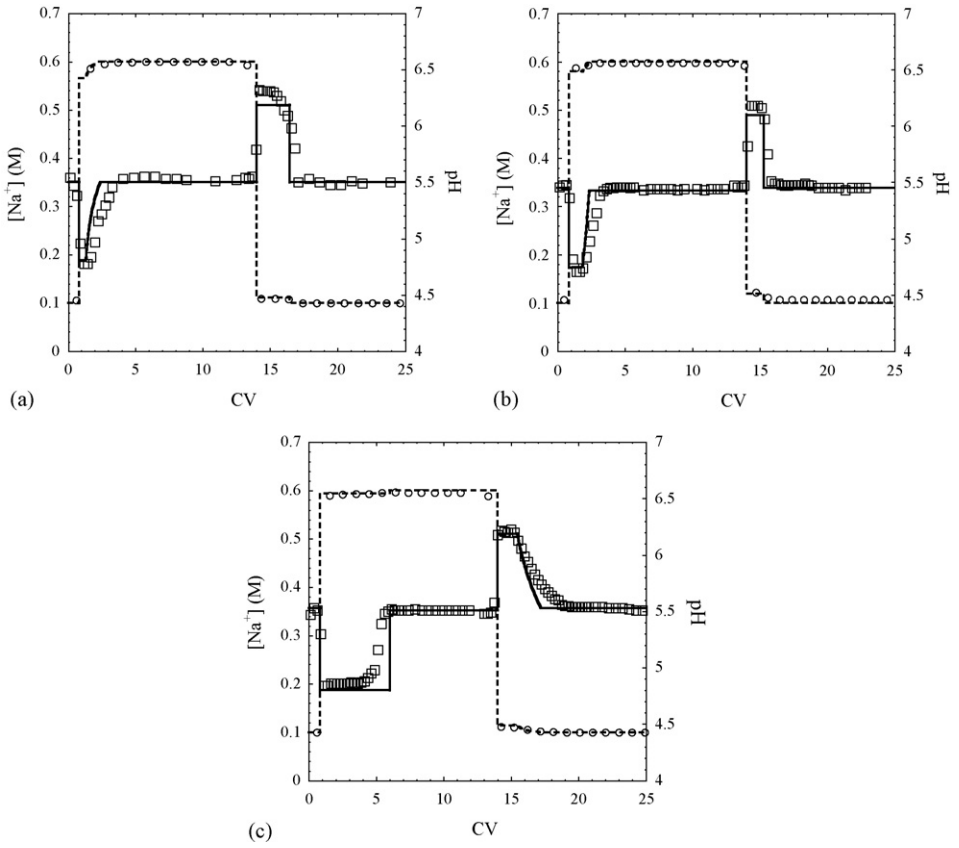

Fig. 5. Experimental and predicted pH and sodium concentration profiles for positive and negative 0–0.5 M NaCl steps with resin A using buffers containing 0.1 M Na^+ at pH 5.5. (a) Acetate, (b) citrate, and (c) phosphate. (◯) Exp. Na^+, (□) exp. pH, (- - - -) model Na^+, (—) model pH.

pK_a-value(s). For resin A the durations of the pH drops were found to be approximately 7.5, 7.5, 2.0, and 34 CV for 0.02 M sodium acetate, citrate, MES, and phosphate buffers, respectively. The significant difference between MES and the other buffers is due mainly to the fact that the zwitterionic form allows for a much higher concentration of buffering species at the same sodium counterion concentration (see Table 1). When comparing the acetate, citrate and phosphate buffers, which all have comparable buffer species concentrations at the same Na^+ concentration, the difference in duration of pH excursions are due to the different buffer pK_a's. Acetate and citrate have pK_a's much closer to the operating pH than does phosphate, thus they have shorter pH transients. The corresponding durations of the pH rises were found to be approximately 3, 6, 1, and 16 CV for 0.02 M sodium acetate, citrate, MES, and phosphate buffers, respectively. For these conditions (initially at high salt) the apparent pK_a is lower due to the ionic strength of the buffer than the no NaCl buffer. Thus, pH excursions are longer for acetate during the positive salt step than it is for the negative one. Phosphate and MES have shorter pH transients for the step

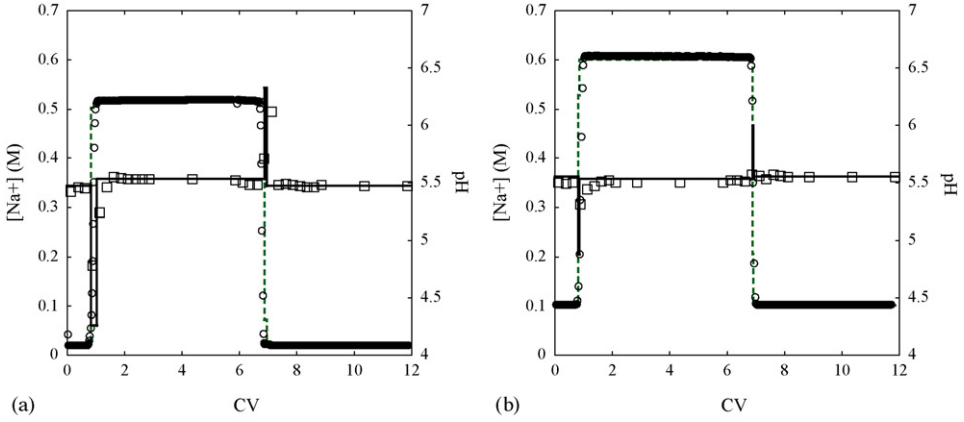

Fig. 6. Experimental and predicted pH and sodium concentration profiles for positive and negative 0–0.5 M NaCl steps with resin C using acetate buffers containing at pH 5.5 containing (a) 0.02 M Na^+ and (b) 0.1 M Na^+. (◯) Exp. Na^+, (□) Exp. pH, (- - - -) model Na^+, (—) model pH.

down than for the step up. Interestingly, the citrate excursions are similar for steps in both directions, as the buffer has three pK_a's all near the operating pH. The same observations can be made for the buffers containing 0.1 M Na^+, although, of course, the durations of these excursions are much shorter.

When comparing the different resins, as expected from the model, resins B and C have much shorter durations than resin A due to the much lower concentration of weak acid groups. For example, the acetate buffer containing 0.02 M Na^+ shows a pH transient duration of 7.5 CV for resin A compared to a duration of only 0.8 CV for resin B and just 0.2 CV for resin C.

4.3. pH transitions for salt gradients

Fig. 7 shows experimental and predicted pH transitions for linear 0–0.5 M NaCl gradients with resin A using acetate, citrate, MES, and phosphate buffers containing 0.02 M Na^+ at pH 5.5. The predicted profiles are based on the local equilibrium model discussed above. However, in this case the model material balance equations (Eqs. (34)–(36) were solved numerically discretizing the axial derivative by backward finite differences. The resulting set of ordinary differential equations was solved using a FORTRAN program available in our laboratory, which utilize subroutine DIVPAG in the IMSL library. Since the discretization introduces numerical dispersion the number of discretization points was kept relatively high to approximate ideal conditions.

As seen in Fig. 7, the model provides again an excellent prediction of the induced pH gradient for all four buffer systems. In all cases, the pH drops sharply at the beginning of the run and gradually returns to the operating pH with a transition extending beyond the duration of the salt gradient. For the phosphate system, the pH minimum occurs much later, after the gradient has reached 0.5 M NaCl, with a shock transition requiring 35–40 CV to return to the operating pH. As in the case of salt steps, the MES buffer provides the best pH control resulting from the zwitterionic nature of this buffer, which allows a high concentration of buffering species with a small counterion concentration. As expected, the pH swings were less pronounced when using the 0.1 MN sodium buffers with the magnitude of the pH drop being not more than 0.25 pH units for any of the buffers (data not shown). The pH transitions were also much less pronounced for resins B and C in gradient mode (data not shown).

4.4. Effects of operating parameters on pH transitions

The predicted effects of various operating parameters on the pH transients with positive and negative salt concentration steps are shown Figs. 8 and 9 for a few different conditions. Fig. 8 shows the effects of the size of the NaCl steps, the buffer concentrations, and the concentrations of weak acid groups in the resin using an acetate buffer containing 0.02 M Na^+ at pH 5.5 and the properties of resin A as a baseline case. As seen in Fig. 8a, both the magnitude and duration of the pH transitions are

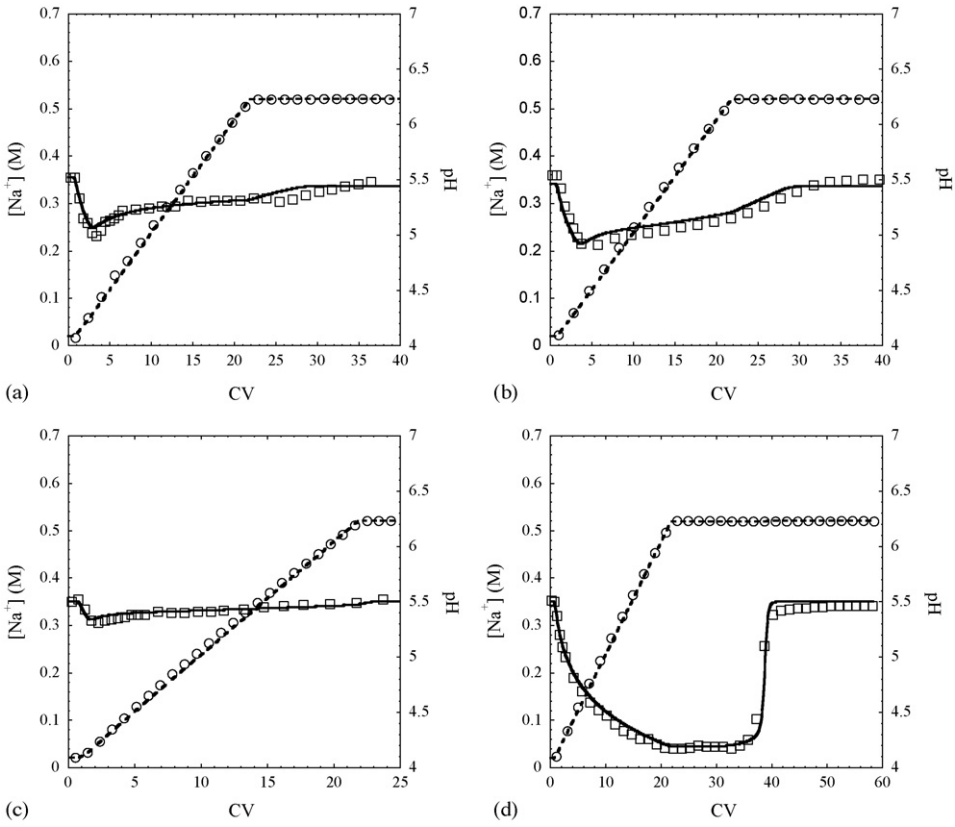

Fig. 7. Experimental and predicted pH and sodium concentration profiles for 0–0.5 M NaCl, 21 CV gradients with resin A using buffers containing 0.02 M Na^+ at pH 5.5. (a) Acetate, (b) citrate, (c) MES, and (d) phosphate. (◯) Exp. Na^+, (□) Exp. pH, (- - - -) model Na^+, (—) model pH.

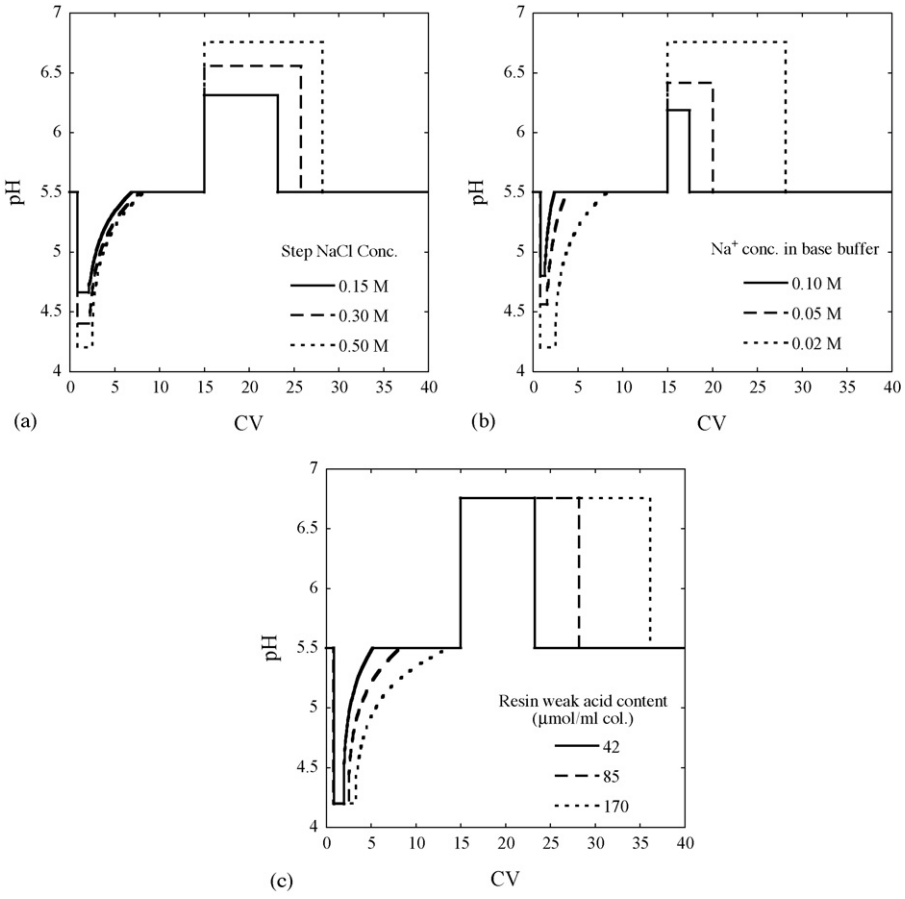

Fig. 8. Predicted effects of operating conditions for NaCl steps using acetate buffers at pH 5.5. Base conditions are: weak acid content of 170 μmol/ml packed column, acetate buffer containing 0.02 M Na^+, 0–0.5 M NaCl steps. (a) Effect of [NaCl] step, (b) effect of buffer concentration (values in legend correspond to [Na^+] in the buffer), and (c) effect of q_R.

decreased when [NaCl] is decreased. Thus, choosing an appropriate NaCl step for desorption of a protein is important. One must choose a high enough NaCl concentration to avoid broad elution peaks and to elute the protein in a timely fashion; however, using NaCl concentrations that are higher than necessary should be avoided. Similarly, as seen in Fig. 8b, increasing buffer strength will decrease the magnitude and duration of pH excursions. However, while choosing a high buffer concentration will reduce the pH transitions, it will also reduce the binding capacity of protein on the resin. Thus, optimal operating conditions must be chosen and careful consideration must be given to the effect on capacity and equilibration and elution time, which both ultimately effect productivity. Finally, the effect of changing q_R is shown in Fig. 8c. As expected, reducing the concentration of weak acid groups decreases the duration of the pH transitions; however, it does not change the magnitude. When screening a resin for use in a particular process, this will not likely be a parameter that can be changed, but it could be the deciding factor between different stationary phase choices. Unfortunately, this decision is not always easy to make since weak acid groups can sometime result in more favorable protein separations and binding capacity [14].

Finally, Fig. 9 shows a comparison of the different buffers for various pH values and two different buffer concentrations with 0–0.5 M NaCl steps. The magnitudes of the pH transitions predicted by the local equilibrium model is nearly the same for all buffers, with the small variation being caused by the different effects of ionic strength on the buffer pK_a-values. However, the duration of the pH drop changes with operating pH. For the acetate buffer, the duration was longest at pH 6.5 and decreased as the operating pH approached the pK_a of acetic acid. The same trend was observed for phosphate buffer—only in reverse. In all cases, MES buffer had the shortest duration, due to the fact that pK_a of the buffer lies in the middle of the range of pH values tested and the concentration of buffering species was highest of all buffers studied. This result is consistent with our experimental results, but is different from the experimental observations of Ghose et al. [1] for the resin Fractogel EMD $SO3^-$. These authors reported larger pH dips for MES than for citrate or phosphate. The reasons for this discrepancy are not clear. A possibility is that the behavior of MES on Fractogel is intrinsically different from that on the resins used in our study. Although the resins are chemically similar, this possibility cannot be ruled out. As suggested by Soto Pérez and Frey [2] it may be possible that the zwitterionic form of MES is adsorbed by the Fractogel resin, thereby influencing the pH transients. Another possibility for the discrepancy could be differences in the way the buffers were actually prepared in the work of Ghose et al. and in our

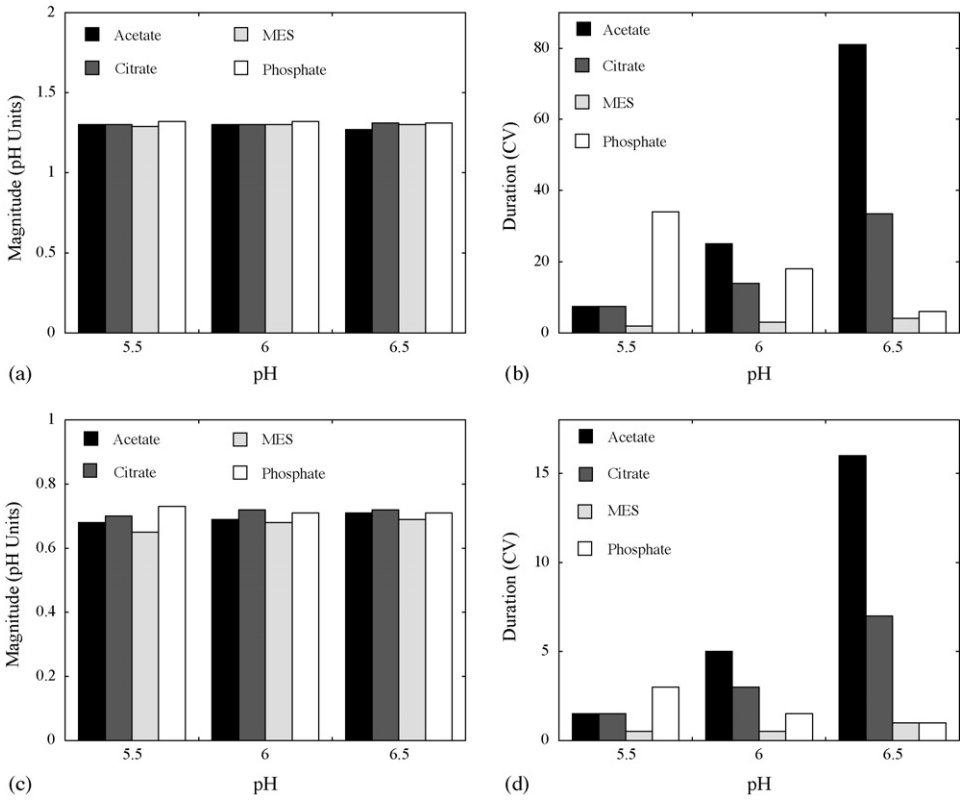

Fig. 9. Predicted pH drops with a 0–0.5 M NaCl step for different buffers using resin A parameters. (a) Magnitude, (b) duration of the pH using buffers containing 0.02 M Na^+, (c) magnitude, and (d) duration of the pH drop using buffers containing 0.1 M Na^+.

study. A final possibility is that band-broadening effects may have partially obscured the individual trends in the magnitude and duration of the pH transients in the work of Ghose et al. For example, if dispersion were substantial it may be possible that an increase in duration may actually manifest itself experimentally as an increase in magnitude of the pH transition. In our work we were able to clearly separate the two trends, although this may not have been possible in the work Ghose et al. who only report the magnitude of the pH dip.

5. Conclusions

A predictive model has been developed to describe pH transitions that occur in columns packed with stationary phases containing weak acid groups. Such pH transitions occur during salt steps and gradients, even when the mobile phase is buffered and the buffering species do not interact with the stationary phase. During positive steps in salt concentration, the pH temporarily decreases before returning to the operating pH. Negative salt steps show the same result, only in reverse. Large salt steps, low buffer concentrations and high concentrations of weak acid groups produce substantial pH swings in these resins. pH fluctuations can alter protein retention and cause problems with pH-sensitive proteins.

Overall the model does an excellent job predicting the shape of the pH waves, and the magnitude and duration of the pH drop associated with step and gradient changes in salt concentrations for three different stationary phases. Not surprisingly, pH fluctuations were milder for resins B and C as a result of a lower concentration of weak acid groups. Also, higher buffer concentrations resulted in smaller pH drops and fewer column volumes to return to the operating pH. MES buffer at pH values in the range of 5.5–6.5 was shown to have the shortest pH excursions of the four buffers tested for positive and negative steps of 0–0.5 M NaCl due to its high concentration of buffering species and since the pK_a of the buffer is closer to the operating pH.

One attractive feature of our model is that the only fitted parameters are those obtained from a single potentiometric titration of the resin. The same parameters can be used to predict the behavior of different buffer systems, at different buffer concentrations, and with different NaCl concentrations in both step and gradient mode.

Acknowledgements

This research was supported by Bio-Rad Laboratories and by NSF Grant no. CTS-0414143.

References

[1] S. Ghose, T.M. McNerney, B. Hubbard, Biotechnol. Prog. 18 (2002) 530.
[2] J. Soto Pérez, D.D. Frey, Biotechnol. Prog. 21 (2005) 902.
[3] B.J. Bennett, F.G. Helfferich, in: D. Naden, M. Streat (Eds.), Ion Exchange Technology, Horwood, Chichester, UK, 1984, pp. 322–330.

[4] R.J. Beynon, J.S. Easterby, Buffer Solutions—The Basics, Oxford University Press, Oxford, 1996.
[5] C.W. Davies, J. Chem. Soc. (1938) 2093.
[6] J.I. Partanen, A.K. Covington, J. Chem. Eng. Data 48 (2003) 797.
[7] J.I. Partanen, A.K. Covington, J. Chem. Eng. Data 50 (2005) 1502.
[8] J.I. Partanen, A.K. Covington, J. Chem. Eng. Data 50 (2005) 2065.
[9] F. Helfferich, Ion Exchange, McGraw-Hill, New York, 1962.
[10] A.V. Stoyanov, P.G. Righetti, J. Chromatogr. A 853 (1999) 35.
[11] F. Helfferich, G. Klein, Multicomponent Chromatography: Theory of Interference, Marcel Dekker, Ann Arbor, 1970.
[12] D.M. Ruthven, Principles of Adsorption and Adsorption Processes, Wiley, 1984.
[13] A.K. Hunter, G. Carta, J. Chromatogr. A 897 (2000) 65.
[14] R. Necina, K. Amatschek, A. Jungbauer, Biotechnol. Bioeng. 60 (1998) 690.